Pharm Res (2013) 30:3045–3058
DOI 10.1007/s11095-013-1104-6

RESEARCH PAPER

Lipid Absorption Triggers Drug Supersaturation at the Intestinal Unstirred Water Layer and Promotes Drug Absorption from Mixed Micelles

Yan Yan Yeap • Natalie L. Trevaskis • Christopher J. H. Porter

Received: 3 March 2013 / Accepted: 4 June 2013 / Published online: 21 June 2013

ABSTRACT

Purpose To evaluate the potential for the acidic intestinal unstirred water layer (UWL) to induce drug supersaturation and enhance drug absorption from intestinal mixed micelles, *via* the promotion of fatty acid absorption.

Methods Using a single-pass rat jejunal perfusion model, the absorptive-flux of cinnarizine and ^{3}H-oleic acid from oleic acid-containing intestinal mixed micelles was assessed under normal acidic microclimate conditions and conditions where the acidic microclimate was attenuated *via* the co-administration of amiloride. As a control, the absorptive-flux of cinnarizine from micelles of Brij® 97 (a non-ionizable, non-absorbable surfactant) was assessed in the absence and presence of amiloride. Cinnarizine solubility was evaluated under conditions of decreasing pH and decreasing micellar lipid content to assess likely changes in solubilization and thermodynamic activity during micellar passage across the UWL.

Results In the presence of amiloride, the absorptive-flux of cinnarizine and ^{3}H-oleic acid from mixed micelles decreased 6.5-fold and 3.0-fold, respectively. In contrast, the absorptive-flux of cinnarizine from Brij® 97 micelles remained unchanged by amiloride, and was significantly lower than from the long-chain micelles. Cinnarizine solubility in long-chain micelles decreased under conditions where pH and micellar lipid content decreased simultaneously.

Conclusions The acidic microclimate of the intestinal UWL promotes drug absorption from intestinal mixed micelles *via* the promotion of fatty acid absorption which subsequently stimulates drug supersaturation. The observations suggest that formulations (or food) containing absorbable lipids (or their digestive precursors) may outperform formulations that lack absorbable components since the latter do not benefit from lipid absorption-induced drug supersaturation.

KEY WORDS absorption · food effect · lipid based formulations · poorly water soluble drug · supersaturation · unstirred water layer

ABBREVIATIONS

CD36	Cluster of Differentiation 36
CIN	cinnarizine
FATP	fatty acid transport protein
GI	gastrointestinal
HPLC	high performance liquid chromatography
LBF	Lipid based formulation
LCFA	long-chain fatty acid
LFCS	Lipid Formulation Classification System
LPC	L-α-lysophosphatidylcholine
OA	oleic acid
PWSD	poorly water-soluble drugs
SEIF	simulated endogenous intestinal fluid
SR-BI	Scavenger Receptor Class B Type I
UWL	unstirred water layer

INTRODUCTION

Co-administration of poorly water-soluble drugs (PWSD) with lipids often leads to a significant enhancement in oral bioavailability (1). In the small intestine, the digestion of formulation or dietary-derived di/triglycerides liberates fatty acids and monoglycerides that are solubilized by biliary components (bile salts, phosphatidylcholine, cholesterol) to generate a series of lipid colloidal species including vesicles and mixed micelles. These colloidal phases provide dispersed lipidic

Electronic supplementary material The online version of this article (doi:10.1007/s11095-013-1104-6) contains supplementary material, which is available to authorized users.

Y. Y. Yeap • N. L. Trevaskis (✉) • C. J. H. Porter (✉)
Drug Delivery, Disposition and Dynamics
Monash Institute of Pharmaceutical Sciences, Monash University
381 Royal Parade Parkville, Victoria 3052, Australia
e-mail: natalie.trevaskis@monash.edu
e-mail: chris.porter@monash.edu

microenvironments for the solubilization of co-administered PWSD, thereby increasing the drug solubilization capacity of the small intestine when compared to the fasted state (2).

Although solubilization increases the apparent solubility of PWSD in the small intestine, and effectively circumvents traditional dissolution, the total concentration of drug in solution (C_{total}) exists in equilibrium between the concentration solubilized in the colloidal fraction ($C_{colloid}$) and the concentration in the free fraction (C_{free}):

$$C_{total} = C_{free} + C_{colloid} \quad (1)$$

In the absence of solid drug, solubilization in colloidal structures such as micelles and vesicles reduces drug thermodynamic activity (3). In simple micellar systems a reduction in thermodynamic activity manifests as a decrease in C_{free}. Thus, solubilization in colloids does not increase (and may reduce) free drug concentrations. Whether increases in total solubilization capacity translate into enhancements in drug absorption is therefore difficult to predict with certainty. Indeed, recent studies suggest that in the absence of an increase in free drug concentrations, solubilization may not result in enhanced drug absorption despite increases in total solubilized drug concentrations (4–6).

Recently, however, we have observed that formulations containing lipids may provide unique absorption benefits for solubilizing formulations, since drug supersaturation appears to be triggered during lipid processing in the gastrointestinal (GI) tract (7–11). Under these circumstances, the induction and maintenance of supersaturation has the potential to reverse (or at least attenuate) the reduction in drug thermodynamic activity inherent in solubilization, and may significantly enhance free drug concentrations above the aqueous solubility. For lipid-based formulations (LBF), drug supersaturation may be generated by several processes. Firstly, when the formulation loses solubilization capacity during the dilution of water miscible co-solvents or surfactants (12–14), secondly, as a result of the digestion of triglycerides and/or surfactants within the formulation (7–9,15), and thirdly as lipid-rich colloidal species are diluted by biliary secretions (10,11).

Enhanced drug absorption resulting from drug supersaturation in lipid-based systems has been described previously using colloidal species modeled on the structures that likely form during the digestion of glyceride lipids (*i.e.* micelles and vesicles comprised of exogenous fatty acid and monoglyceride solubilized in endogenous bile salts, lysophospholipid and cholesterol) (10,11). In these studies, interaction of secreted bile with lipid colloidal phases reduced the solubilization capacity of the colloids for some poorly water-soluble weak bases, but since drug precipitation was not immediate, supersaturation was induced. The period of drug supersaturation that preceded drug precipitation coincided with significant enhancements in the absorption of cinnarizine across rat jejunum (10,11).

Interestingly, in the same studies, some increase in absorption in the presence of bile was also apparent for danazol, even though interaction with bile did not reduce micellar solubilization capacity *in vitro* (and therefore did not stimulate supersaturation). Indeed, addition of bile increased drug solubility in a fashion more consistent with traditional models for micellar solubilization (where the addition of solubilizing species such as bile typically increases solubilization capacity). For danazol, the driver for increased drug absorption was suggested to be the potential for lipid absorption (*i.e.* the removal of micellar lipid content) to reduce micellar drug solubilization capacity and to trigger drug supersaturation at the absorptive site (assuming lipid absorption is faster than drug absorption). This concept has been examined in more detail here.

The absorption of long-chain fatty acids (LCFA) is facilitated by an acidic microclimate (pH 5.3–6.2 (16–19)) that is present within the unstirred water layer (UWL) (19,20). The UWL (see Fig. 1) separates bulk intestinal fluid from the surface of intestinal absorptive cells, and is ~500–800 μm wide (17,18). The UWL exists coincident with, and is indistinguishable from, a viscous mucus layer consisting of water (~ 95%), glycoproteins, lipids, mineral salts and free proteins (17,21,22). The acidic microclimate of the UWL is maintained by the action of the Na^+/H^+ antiporter at the brush border membrane (18), as well as the mucus coating which retards H^+ diffusion into bulk luminal fluid (17,18). Shiau and colleagues were the first to describe the facilitatory role of the acidic microclimate in dietary LCFA absorption from intestinal mixed micelles (20). These studies showed that LCFA absorption was higher in the presence of the low pH microclimate of the UWL. The authors postulated that the exposure of micelles to the UWL acidic microclimate led to the protonation of ionized LCFA, and subsequently increased lipid absorption *via* two mechanisms (depicted in Fig. 1(i)). Firstly, protonated LCFA were expected to preferentially partition into and across the absorptive membrane in accord with classical pH-partition theory (19,20). Secondly, the protonation of fatty acids was suggested to reduce LCFA amphiphilicity and thereby reduce LCFA solubility in bile salt micelles. The decrease in micellar LCFA solubility was suggested to stimulate micellar dissociation, resulting in increased LCFA thermodynamic activity and increased absorption. A decrease in pH at the UWL is therefore expected to lead to a reduction in the lipid content of intestinal mixed micelles *via* promotion of LCFA micellar dissociation and absorption (Fig. 1(i)).

Since the presence of lipid digestion products within mixed micelles contributes significantly to drug solubilization capacity (11,15,23), in the current submission we have explored the hypothesis that in promoting LCFA micellar

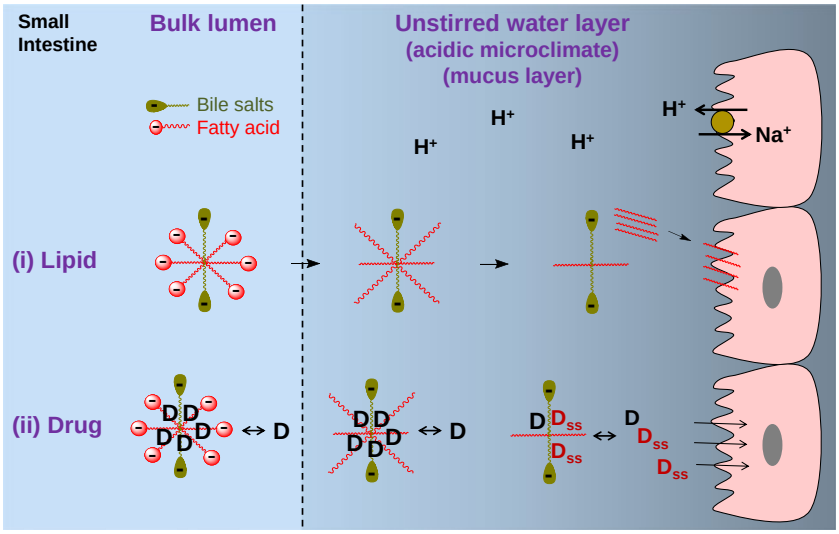

Fig. 1 Schematic of the proposed mechanisms by which the UWL acidic microclimate facilitates the absorption of micellar solubilized (*i*) long-chain fatty acids (LCFA, shown in *red*) and (*ii*) poorly water-soluble drug (D). (*i*) Exposure of mixed micelles to the acidic microclimate leads to protonation of LCFA, attenuates their amphiphilic character and reduces LCFA solubility in mixed micelles. Increased LCFA thermodynamic activity subsequently promotes LCFA dissociation from mixed micelles and absorption across the apical membrane. Protonated LCFA is also expected to partition more readily across the lipophilic absorptive membrane. (*ii*) At the UWL, removal of LCFA from mixed micelles *via* dissociation and absorption decreases the solubilization capacity for drug (D), therefore triggering drug supersaturation in close proximity to the absorptive site, and enhancing D absorption *via* increases in thermodynamic potential. D is either free and available for absorption or associated with micelles. D_{ss} signifies acidic microclimate-induced drug supersaturation that drives increases in D absorption.

dissociation and absorption, the acidic microclimate also promotes a reduction in the drug solubilization capacity of LCFA-containing intestinal mixed micelles. This is expected to facilitate drug absorption *via* the induction of drug supersaturation at the UWL.

The data suggest that lipid absorption is a significant trigger for the induction of drug supersaturation, and that the combination of fatty acid-containing solubilizing species and the acidic intestinal unstirred water layer may be a particularly powerful driver for drug supersaturation and absorption. The results provide an improved mechanistic understanding of the enhancement in drug absorption often observed from lipid-based systems containing digestible lipids, and also serve to further explain the beneficial effects of digestible lipids in food on drug absorption.

MATERIALS AND METHODS

Materials

Cinnarizine, flunarizine dihydrochloride, amiloride hydrochloride hydrate, sodium taurocholate, sodium taurodeoxycholate, sodium glycocholate, sodium glycochenodeoxycholate, cholesterol, L-α-lysophosphatidylcholine (LPC, from egg yolk), oleic acid, sodium chloride (NaCl) and Brij® 97 were obtained from Sigma-Aldrich, Australia. Sodium taurochenodeoxycholate, sodium glycodeoxycholate, ortho-phosphoric acid 85% (H_3PO_4), sodium hydroxide pellets (NaOH) and *tert*-butyl methyl ether (TBME) were from Merck, Australia. Disodium hydrogen orthophosphate (Na_2HPO_4), sodium dihydrogen orthophosphate ($NaH_2PO_4.2H_2O$) and ammonium dihydrogen orthophosphate ($NH_4H_2PO_4$) (Ajax Finechem, Australia), Irga-Safe Plus™ (Perkin Elmer Life Sciences, MA), oleic acid, [9,10-^{3}H(N)] (60 Ci/mmol) (American Radiolabeled Chemicals, MO), transcutol HP (Gattefossé, France), heparin sodium injection BP (1,000 I.U./mL, Hospira, Australia), xylazine (100 mg/mL, Troy Laboratories, Australia), acepromazine (10 mg/mL, Ceva Delvet, Australia), ketamine (100 mg/mL, Provet, Australia) and pentobarbitone sodium (325 mg/mL, Virbac, Australia) were obtained from listed suppliers. Acetonitrile and chloroform used were analytical reagent grade. Water was obtained from a Millipore milliQ Gradient A10 water purification system (Millipore, MA).

Experimental Outline

In situ rat jejunal perfusion experiments with simultaneous mesenteric blood collection were conducted to assess the role of the acidic microclimate in LCFA and drug absorption from LCFA-containing intestinal colloids. Specifically, the intestinal absorptive flux of oleic acid and cinnarizine from a model LCFA-containing colloid ("model LCFA colloids") was assessed in the absence and presence of 2 mM amiloride. Amiloride is a competitive inhibitor (with respect to Na^+) of the plasma membrane Na^+/H^+ exchanger (24) and has previously been shown to attenuate the acidic microclimate on the cell surface of the rat jejunum (18). Amiloride was

therefore used as an inhibitor of fatty acid absorption. As a control, the absorption of cinnarizine from "model Brij 97 colloids" (Brij 97 is a non-ionizable and non-absorbable surfactant) in the absence and presence of 2 mM amiloride was also assessed. The total cinnarizine concentration (130 μg/mL) and cinnarizine thermodynamic activity (~ 80% saturated solubility) were matched in both colloidal systems. Cinnarizine (a weak base) was selected as a model PWSD, as cinnarizine solubility in LCFA-containing colloids is highly dependent on oleic acid content (11), and therefore may be more amenable to enhancement in drug thermodynamic activity induced by LCFA absorption. Exposure to UWL microenvironment acidity is also expected to increase cinnarizine ionization, and therefore decrease drug absorption based on pH partition relationships. As such, any increase in drug absorption that occurs due to microenvironment acidity is expected to reflect mechanisms unrelated to drug ionization/partitioning. The model LCFA colloids used in this study were chosen to be representative of the post-digestion lipid colloidal phases likely responsible for the presentation of solubilized drug to the absorptive membrane (2,23).

In vitro solubility studies were conducted to evaluate expected changes in cinnarizine solubilization when model LCFA or Brij 97 colloids are exposed to the acidic microclimate *in vivo*. The equilibrium solubility of cinnarizine was assessed in a series of LCFA colloids with decreasing system pH and decreasing lipid concentration (to simulate exposure to the acidic microclimate and lipid absorption); as well as in a series of Brij 97 colloids with decreasing system pH (to simulate exposure to the acidic microclimate *only*, as Brij 97 is not absorbed).

The role of the acidic microclimate in the absorption of cinnarizine from supersaturated, LCFA-containing colloids was also assessed in rat jejunal perfusion studies *via* co-perfusion of donor bile with cinnarizine-loaded LCFA colloids (conditions previously shown to induce cinnarizine supersaturation *in situ* and to promote intestinal drug absorption (11)), in the absence and presence of 2 mM amiloride.

Preparation of LCFA-Containing Intestinal Colloids

The model LCFA colloids used in *in situ* rat perfusion studies comprised 0.1% w/v oleic acid and 0.06% w/v monoolein solubilized in simulated endogenous intestinal fluid (SEIF) (23) at pH 6.30±0.01. SEIF comprised 4 mM total bile salt (25 mol% glycocholate, 17.5 mol% glycodeoxycholate, 25 mol% glycochenodeoxycholate, 12.5 mol% taurocholate, 7.5 mol% taurodeoxycholate, 12.5 mol% taurochenodeoxycholate), 1 mM LPC and 0.25 mM cholesterol. The oleic acid:monoolein molar ratio was kept at 2:1, reflecting the ratio of digestion products expected from digestion of 1 mole of triolein. To model the effect of colloid interaction with the acidic microclimate and the absorption of lipid components on cinnarizine solubility, systems were prepared at decreasing pH (pH 6.3, 5.8, 5.3, 4.8) and with decreasing quantities of lipids (0.1, 0.05, 0.025, 0% w/v oleic acid, with a proportional decrease in monoolein concentrations) for cinnarizine equilibrium solubility determinations.

SEIF and LCFA colloids were prepared as described previously (11). pH adjustment of colloids to 6.30, 5.80, 5.30, 4.80 was achieved by drop wise addition of H_3PO_4. To prepare drug-loaded LCFA colloids (for *in situ* jejunal perfusion studies), cinnarizine was pre-dissolved in oleic acid and allowed to equilibrate overnight at a concentration of 61 mg/g and 115 mg/g to allow generation of colloids containing 65 μg/mL (~ 40% saturated solubility) and 130-μg/mL (~ 80% saturated solubility) cinnarizine. As a final step, trace quantities of ^{3}H-oleic acid (0.25 μCi/mL) were added to the drug-loaded colloids, followed by a 1-min vortex. When amiloride was included in the LCFA colloids, the appropriate mass of amiloride was dissolved in the prepared colloids at 37°C, and used within 30 min of preparation. The sodium concentration in all prepared colloids was 150 mM.

Preparation of Brij 97 Colloids

Brij 97 (a liquid at 37°C) was weighed into a volumetric flask and made to volume with phosphate buffer (18 mM $NaH_2PO_4.2H_2O$, 12 mM Na_2HPO_4, 108 mM NaCl), followed by pH adjustment to 6.30±0.01 with H_3PO_4. From a plot of cinnarizine solubility *vs.* Brij 97 concentration, 3.09% w/v Brij 97 was identified as the concentration required to provide equal cinnarizine solubilization capacity as the model LCFA colloid (*i.e.* 157.7 μg/mL). This concentration (3.09% w/v) was therefore used to form the model Brij 97 colloids that were used in jejunal perfusion experiments. Solutions of 3.09% w/v Brij 97 were also prepared at pH 5.80, 5.30, 4.80 (pH adjustment *via* drop wise addition of H_3PO_4 solution) for cinnarizine equilibrium solubility determinations. For the preparation of drug-loaded Brij 97 colloids (for *in situ* jejunal perfusion studies), 100 μL of a 130 mg/mL cinnarizine in transcutol stock solution was spiked into 10 mL of model Brij colloids to achieve a final concentration of 130 μg/mL cinnarizine (~ 80% saturated solubility). When amiloride was included in the Brij 97 colloids, the appropriate mass of amiloride was dissolved in the prepared colloids at 37°C, and used within 30 min of preparation. The sodium concentration in all colloids was 150 mM.

Equilibrium Solubility Studies of Cinnarizine in Colloids

The equilibrium solubility of cinnarizine in LCFA colloids and Brij 97 colloids was determined as described previously

(10). The equilibrium solubility of cinnarizine was also determined when 2 mM amiloride was included in model LCFA colloids, model Brij 97 colloids, and 1:1 v/v mixtures of model LCFA colloids and fasted rat bile, to confirm that cinnarizine solubilization capacity was unaltered by amiloride (data not shown). Based on physical examination and the maintenance of consistent drug solubilization capacity, model LCFA and Brij 97 colloids were stable for 5 days.

For some LCFA colloids at pHs<5.8, phase separation into a highly dispersed aqueous phase and an undispersed oil phase was evident. Since an oil phase is not likely to be retained at the UWL *in vivo* (unionized LCFA is expected to be readily absorbed), the drug solubilization capacity of the aqueous micellar phase rather than the oil phase was deemed relevant in assessing expected changes to drug solubilization and thermodynamic activity in the UWL. To accurately determine the equilibrium solubility of cinnarizine in the aqueous phase for all LCFA colloids, solubility samples were left to equilibrate at 37°C for 120 h (as equilibrium solubility was attained by this time), and ultracentrifuged for 30 min at 37°C and 400,000×*g* (Optima xL-100 K centrifuge, SW-60 rotor, Beckman, Palo Alto, CA) to separate samples into an aqueous phase, an undispersed oil phase (if any), and a pellet phase (containing excess solid drug) as described previously (25). Samples from the aqueous phase were assayed for cinnarizine content by HPLC.

Animals

All rat studies were approved by the institutional animal ethics committee, and were conducted in accordance with the guidelines of the Australian and New Zealand Council for the Care of Animals in Research and Teaching. Male Sprague–Dawley rats (280–330 g) were used in all experiments, and were allowed to acclimatize in the institutional animal housing facility for at least 7 days with free access to standard chow and water. All animals were fasted overnight (12–18 h) prior to surgery.

Surgical Procedures

Anaesthesia was induced and maintained as described previously (10). Rats were maintained on a 37°C heated pad throughout surgery and experiments and ultimately euthanized *via* an intravenous or intracardiac injection of 100 mg sodium pentobarbitone.

Single-Pass Rat Jejunum Perfusion

Absorptive flux across rat jejunum was assessed using *in situ* perfusion (single-pass) of an isolated jejunal segment (~ 10 cm) and simultaneous blood collection from the corresponding mesenteric vein branch as described previously (10).

Fasted Rat Bile Collection

Fasted bile from donor rats was collected as described previously (10).

Intestinal Absorptive Flux Assessment *Via In Situ* Single-Pass Rat Jejunum Perfusion

After surgery, animals were equilibrated for 30-min as described previously (10). For experiments where amiloride was administered, perfusion buffer containing 2 mM amiloride was perfused during the equilibration period. Perfusate flow through the jejunal segment was 0.1 mL/min to minimize variations in the thickness of the unstirred water layer (as this may influence drug flux (26)). Following the equilibration period, perfusion buffer was replaced with model colloids. The perfused colloids were sampled at $t=0$ to confirm cinnarizine and/or ^{3}H-oleic acid concentrations. After this time, the outflowing perfusate was continuously collected at 10-min intervals, and vortexed before analysis of drug and/or ^{3}H-oleic acid content. Blood draining the perfused jejunal segment was collected at 5-min intervals, plasma separated by centrifugation (10,000 ×*g*, 5 min), and samples analysed for cinnarizine and/or ^{3}H-oleic acid.

The concentration of cinnarizine flowing into the perfused jejunal segment was held at 130 μg/mL in studies assessing the role of the acidic microclimate in the absorption of cinnarizine from model LCFA-containing or Brij 97 colloids. When amiloride was included in these experiments, it was predissolved in the model colloids at 37°C at a concentration of 2 mM amiloride. In studies that assessed the role of the acidic microclimate in the absorption of cinnarizine from *supersaturated* LCFA-containing colloids (*i.e.* where co-perfusion of donor rat bile triggered drug supersaturation), the concentration of cinnarizine flowing into the perfused jejunal segment was held at 65 μg/mL. Therefore, in experiments where model colloids were perfused alone, cinnarizine was loaded into the perfusate at 65 μg/mL (~ 40% saturated solubility). In experiments where model colloids were co-perfused in a 1:1 v/v ratio with a secondary perfusate of bile, cinnarizine was loaded into the primary perfusate at 130 μg/mL (~ 80% saturated solubility), such that 1:1 v/v dilution led to a final perfusate concentration of 65 μg/mL cinnarizine. When amiloride was included, it was pre-dissolved in bile at 37°C at 4 mM, such that 1:1 v/v dilution led to a final perfusate concentration of 2 mM amiloride. Both model LCFA colloids and bile were pumped at 0.05 mL/min, and mixed *via* a three-way "T" connector immediately prior to entry into the jejunal segment, such that total perfusate flow was maintained at 0.1 mL/min. Since luminal cinnarizine supersaturation was generated in these experiments, outflowing perfusate samples were taken before and after centrifugation (2,200 ×*g*, 2 min), to obtain an

indication of the degree of drug precipitation within the jejunal segment.

Analytical Procedures

Sample Preparation and HPLC Assay Conditions for Cinnarizine

Samples of LCFA colloids and Brij 97 colloids were prepared for HPLC assay by a minimum 20-fold dilution with mobile phase (50% v/v acetonitrile:50% v/v 20 mM $NH_4H_2PO_4$). Plasma samples were prepared for HPLC as reported previously (10). Replicate analysis of $n=4$ quality control samples revealed acceptable accuracy and precision (± 10%, ± 15% at the limit of quantification) for cinnarizine concentrations between 20–1,000 ng/mL for colloids, and 10–320 ng/mL for plasma.

Scintillation Counting

Quantification of ^{3}H-oleic acid in perfusate and collected plasma was performed *via* scintillation counting on a Packard Tri-Carb 2000CA liquid scintillation analyzer (Packard, Meriden, CT). Perfusate samples (100 μL) and plasma samples (200 μL) were added to 2 mL Irga-safe Plus scintillation fluid followed by a 10-sec vortex. Samples were corrected for background radioactivity by the inclusion of a blank sample in each run. The counting method was validated by spiking blank plasma with low, medium and high concentrations of labeled oleic acid (in triplicate). The measured concentrations were within 5% of nominal.

Blood:Plasma Ratio Determination for Cinnarizine, Oleic Acid

Blood:plasma ratios for cinnarizine and oleic acid have been determined previously (11) and were used to convert plasma concentrations to blood concentrations in perfusion experiments, enabling quantification of total compound transport into mesenteric blood.

Calculations

Permeability coefficients were calculated from flux data obtained after attainment of steady state drug transport into mesenteric blood. Two apparent permeability coefficients (P_{app}) were calculated as described previously (27):

$$'\text{Disappearance}'\ P_{app} = -\frac{Q}{A}\cdot \ln\frac{C_1}{C_0} \tag{2}$$

$$'\text{Appearance}'\ P_{app} = \frac{\left(\Delta M_B / \Delta t\right)}{A < C >} \tag{3}$$

where 'Disappearance' P_{app} is the apparent permeability coefficient calculated from drug loss from the perfusate (cm/sec); 'Appearance' P_{app} is the apparent permeability coefficient calculated from drug appearance in the mesenteric blood (cm/sec); Q is the perfusate flow rate (mL/sec); A is the surface area of the perfused jejunal segment (cm^2), which is calculated by multiplying the diameter and the length of the perfused intestinal segment as described previously (28); C_1 is the average steady state drug concentration exiting the perfused jejunal segment (ng/mL); C_0 is the drug concentration entering the jejunal segment (ng/mL); $\Delta M_B/\Delta t$ is the average rate of drug mass appearance in mesenteric blood at steady state (ng/sec); and $<C>$ is the logarithmic mean drug concentration in the lumen (ng/mL), where $<C> = (C_1 - C_0)/(\ln C_1 - \ln C_0)$.

Statistical Analysis

Statistically significant differences were determined by ANOVA followed by Tukey's test for multiple comparisons at a significance level of $\alpha=0.05$ using SPSS v19 for Windows (SPSS Inc., Chicago, IL).

RESULTS

Attenuation of the Acidic Microclimate Using Amiloride Reduces Oleic Acid and Cinnarizine Absorption from Model LCFA Colloids But Has No Effect on the Absorption of Cinnarizine from Fatty Acid-Free Brij 97 Colloids

Figure 2 shows the intestinal absorptive flux *vs.* time profiles of oleic acid (from LCFA containing colloids), and cinnarizine (from both LCFA and Brij 97 colloids) in the absence and presence of 2 mM amiloride. Corresponding steady state-absorptive flux, disappearance P_{app}, and appearance P_{app} data are reported in Table I. Perfusate disappearance profiles are included in the Supplementary Material (Figure S1).

Administration of amiloride reduced the absorption of oleic acid, resulting in a significant ($p<0.05$) 3.0-fold, 1.4-fold, and 3.0-fold reduction in absorptive flux, disappearance P_{app}, and appearance P_{app} of oleic acid, respectively (Fig. 2a, Table I). Amiloride administration also led to a significant reduction in cinnarizine absorption from LCFA colloids, resulting in 6.5-fold, 2.8-fold, and 5.7-fold reductions ($p<0.05$) in the absorptive flux, disappearance P_{app}, and appearance P_{app} of cinnarizine, respectively (Fig. 2b, Table I). In contrast, co-administration of amiloride with Brij 97 colloids did not lead to significant changes in the absorptive flux, disappearance P_{app}, and appearance P_{app} of cinnarizine (Fig. 2c, Table I).

The model colloids were chosen such that the cinnarizine solubilization capacity in each was the same (157.7 ± 3.0 μg/mL

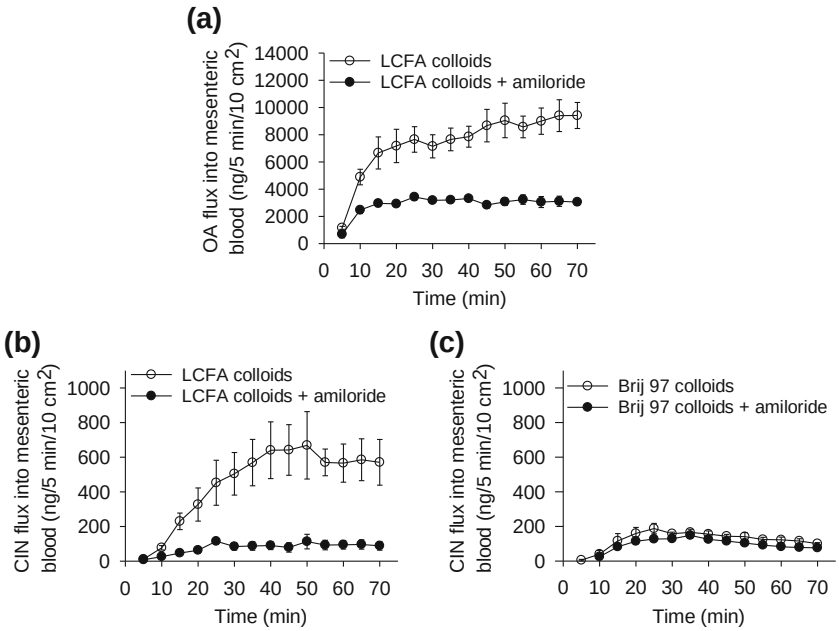

Fig. 2 Mesenteric blood appearance profiles of (**a**) oleic acid (OA) from model LCFA colloids, (**b**) cinnarizine (CIN) from model LCFA colloids, and (**c**) cinnarizine (CIN) from model Brij 97 colloids, after 70 min single-pass perfusion of ~ 10 cm^2 segments of rat jejunum with and without co-administration of 2 mM amiloride. Amiloride was used to attenuate the acidic microclimate of the intestinal unstirred water layer. Model LCFA colloids and model Brij 97 colloids had equal solubilization capacity for CIN (157.7 ± 3.0 μg/mL and 153.2 ± 2.5 μg/mL, respectively; average ± SEM of $n = 3$ determinations). CIN was loaded into both colloids at constant concentration (130 μg/mL) and thermodynamic activity (~ 80% saturated solubility). Data represent mean ± SEM of $n = 3$–4 experiments. Steady state-absorptive flux, disappearance P_{app}, and appearance P_{app} of CIN and OA from this series of experiments are tabulated in Table I.

and 153.2 ± 2.5 μg/mL for LCFA colloids and Brij 97 colloids respectively, mean ± SEM of n = 3 determinations), and drug was loaded at the same concentration (130 μg/mL). Cinnarizine thermodynamic activity was therefore also matched and cinnarizine was dissolved at ~ 80% saturated solubility in both colloidal solutions. In the absence of amiloride (*i.e.* in the presence of an intact acidic microclimate), the absorptive flux of cinnarizine from the LCFA colloids was 4.9-fold higher than from Brij 97 colloids (Fig. 2b and c, Table I). This difference was abolished in the presence of amiloride (*i.e.* under conditions where the acidic microclimate was attenuated and lipid absorption inhibited). The data suggest that cinnarizine absorption is significantly more efficient from LCFA-containing intestinal colloids than from Brij 97 colloids, in spite of matched initial thermodynamic activity in both colloids, and that this is dependent on the presence of an acidic microclimate at the intestinal UWL. For the model LCFA colloids, the increase in cinnarizine absorption in the absence of amiloride also occurred coincidentally with an increase in oleic acid absorption (Fig. 2a, b, Table I).

Table I Cinnarizine (CIN) and Oleic Acid (OA) Disappearance P_{app} (× 10^6 cm/sec) from the Intestinal Perfusate, Appearance P_{app} (× 10^6 cm/sec) in the Mesenteric Blood, and Steady State Absorptive Flux into Mesenteric Blood (ng/5 min/10 cm^2) after 70 min of Single-Pass Perfusion of ~ 10 cm^2 Segments of Rat Jejunum with Model Long-Chain Fatty Acid (LCFA) Colloids or Model Brij 97 Colloids, with and without Co-administration of 2 mM Amiloride. Values Calculated Using Data Obtained After Steady State Attainment ($t = 55$–70 min). Data Represent Mean ± SEM of $n = 3$–4 Experiments

	Perfusate	CIN conc. (μg/mL)	OA conc. (μg/mL)	Disappearance P_{app} (× 10^6 cm/sec)	Appearance P_{app} (× 10^6 cm/sec)	Mesenteric blood flux (ng/5 min/10 cm^2)
CIN	LCFA colloid	130	–	35.5 ± 2.2	1.7 ± 0.4	600 ± 129
	LCFA colloid + amiloride	130	–	12.7 ± 4.1 [a]	0.3 ± 0.1 [a]	93 ± 25 [a]
	Brij 97 colloid	130	–	14.0 ± 6.7 [a]	0.3 ± 0.0 [a]	123 ± 14 [a]
	Brij 97 colloid + amiloride	130	–	5.4 ± 1.2 [a]	0.2 ± 0.0 [a]	90 ± 3 [a]
OA	LCFA colloid	–	1000	22.1 ± 2.0	3.3 ± 0.4	9144 ± 991
	LCFA colloid + amiloride	–	1000	15.3 ± 0.9 [b]	1.1 ± 0.1 [b]	3045 ± 304 [b]

[a] Significantly different ($p < 0.05$) from model LCFA colloid group (containing 130 μg/mL CIN) in the absence of amiloride

[b] Significantly different ($p < 0.05$) from model LCFA colloid group (containing 1,000 μg/mL OA) in the absence of amiloride

Exposure of Model LCFA Colloids to the Acidic Microclimate, and Absorption of Lipid Components, Leads to Cinnarizine Supersaturation and Enhanced Thermodynamic Activity

To examine the possible mechanisms by which pH change and lipid absorption at the UWL affect cinnarizine absorption, the equilibrium solubility of cinnarizine in LCFA colloids was assessed under conditions of decreasing pH and decreasing lipid concentration (Fig. 3a). Equivalent data were also generated for Brij 97 colloids, in this case with decreasing system pH *only*, as Brij 97 is not absorbed (Fig. 3b). As system pH decreased, the LCFA colloids became increasingly turbid, ultimately leading to phase separation into an aqueous phase and an undispersed oil phase (Figure S2). Phase separation occurred earlier (*i.e.* at higher pHs) in systems containing higher concentrations of lipid. Systems that phase separated are asterisked in Fig. 3a. Phase separation occurred at pH 4.8 for all LCFA-based colloids and at and below pH 5.3 for colloids containing the highest lipid load (*i.e.* 0.1% w/v oleic acid). Even where phase separation did not occur, the turbidity of the LCFA colloidal solutions increased with increasing lipid concentration. Development of turbidity was not evident in SEIF (*i.e.* 0% oleic acid) or the Brij 97 colloids (Figure S2).

Changes in turbidity of the LCFA-containing colloids appeared to correlate with changes to solubilization capacity, such that drug solubility was higher in systems with increasing turbidity. As depicted in Fig. 3a, cinnarizine solubility in LCFA colloids increased significantly with increasing lipid concentration and also increased (albeit more moderately) with decreasing pH. These trends continued until phase separation occurred, at which point cinnarizine solubility in the micellar phase was reduced due to partitioning of lipids from the micellar phase into a poorly dispersed lipid phase. At 0% incorporated lipid (*i.e.* SEIF only), cinnarizine solubility also increased slightly with decreasing pH. However, this increase was small when compared to the increase in solubility afforded by increasing lipid concentration or decreasing pH in the LFCA-containing colloids.

In vivo, exposure of LCFA colloids to the intestinal acidic microclimate results in a decrease in pH and an increase in LCFA absorption. Changes to cinnarizine solubility under the same circumstances are therefore expected to be predicted by assessment of solubility changes under conditions where system pH and lipid concentration are decreased simultaneously. 'O' in Fig. 3 identifies the maximum cinnarizine solubilization capacity of the LCFA and Brij 97 colloids at pH 6.3. Cinnarizine was loaded into model colloids at 80% saturated solubility, *i.e.* 130 µg/mL – blue

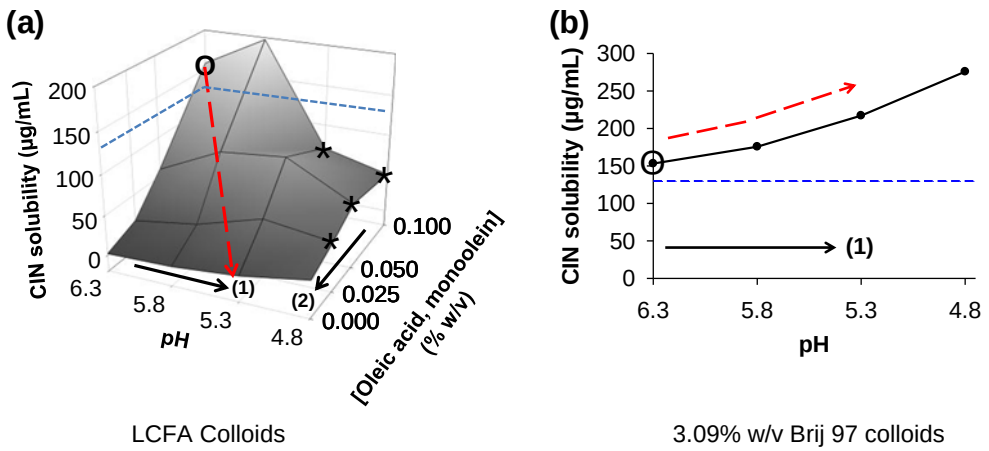

Fig. 3 (**a**) Three-dimensional plot of cinnarizine (CIN) solubility (37°C) in the aqueous phase of LCFA-containing intestinal colloids as a function of oleic acid and monoolein concentration in bile micelles (concentration on y-axis refers to oleic acid concentration) and system pH. The concentration of bile components in (**a**) was kept constant. *Black solid arrows* depict the expected change in CIN solubilization capacity when (1) colloids are exposed to the acidic microclimate of the UWL, and (2) as oleic acid and monoolein are absorbed and removed from colloids (absorption of colloidal components only applies to LCFA colloids as Brij 97 is non-absorbable). * in (**a**) denotes colloidal systems where phase separation into an aqueous phase and undispersed oil phase was evident during the 120 h equilibrium solubility determination study (see Figure S2). 'O' denotes the solubilization capacity of the model LCFA and Brij 97 colloids used in Fig. 2, and the blue dotted line shows the concentration of CIN (*i.e.* 130 µg/mL – 80% saturated solubility) in the model colloids used in Fig. 2 and Table I. The *red broken arrows* depict the theoretical solubility trend when the pH of the system is reduced by 1 unit to pH 5.3 (lowest pH reported in the UWL (17)) and lipids are completely removed. (**b**) CIN solubility (37°C) in 3.09% w/v Brij 97 colloids as a function of system pH. The *red broken arrow* again shows the effect of reducing the pH of the system by 1 unit to pH 5.3 such as on entry into the UWL. The passage of model LCFA colloids across the UWL and subsequent absorption of lipid digestion products is therefore expected to reduce cinnarizine solubility, leading to supersaturation, enhanced thermodynamic potential and absorption. In contrast, the passage of model Brij 97 colloids across the UWL leads to a small increase in CIN solubility and reduced thermodynamic potential.

dotted line. At the highest lipid load (0.1% w/v OA), exposure of the LCFA containing colloids to decreases in pH consistent with conditions in the acidic microclimate, initially increased cinnarizine solubility (at pH 5.8), but ultimately reduced cinnarizine solubility (at pH 5.3, the lowest reported microclimate pH (17)) (Fig. 3). The solubility of cinnarizine was also highly dependent on the concentration of incorporated lipids, and a reduction in oleic acid content (consistent with the reductions expected on lipid absorption) significantly reduced cinnarizine solubility. Indeed, the drop in cinnarizine solubility seen at pH 5.3 most likely reflects a loss of micellar lipid content due to phase separation rather than an effect of pH alone. A theoretical line in Fig. 3a (red broken arrow) depicts the changes in cinnarizine solubility expected under conditions where pH is reduced to pH 5.30 and lipids are fully absorbed. Under these circumstances, cinnarizine solubility is reduced dramatically, and in the absence of precipitation, is expected to lead to supersaturation, enhanced thermodynamic activity and improved absorption.

Conversely, in Brij 97 colloids, a decrease in system pH led to *increased* cinnarizine solubility (Fig. 3b), presumably due to increased cinnarizine ionization at lower pH. Since Brij 97 is not absorbed, the concentration of micellar surfactant is expected to remain constant during passage across the UWL, and the only driver of changes to drug solubility at the UWL is the reduction in pH due to the acidic microclimate. As depicted by the red broken arrow in Fig. 3b, cinnarizine solubilization is therefore expected to increase during passage of Brij 97 colloids across the UWL, leading to reduced thermodynamic activity.

Attenuation of the Acidic Microclimate Using Amiloride Abolishes Bile-Induced, Supersaturation-Enhanced, Cinnarizine Absorption from Model LCFA Colloids

In a recent study (11) co-perfusion of fasted rat bile with cinnarizine-loaded model LCFA colloids triggered cinnarizine supersaturation in the GI lumen and enhanced cinnarizine absorptive flux by 3.2-fold in an *in situ* rat jejunal perfusion model (Fig. 4b, Table II). In the current work, inclusion of 2 mM amiloride in the same perfusate (*i.e.* 1:1 v/v mixture of model LCFA colloids and fasted rat bile) reduced the absorptive flux and appearance P_{app} of oleic acid by 4.6-fold and 4.4-fold, respectively (Table II, Fig. 4a). A coincident decrease in the absorptive flux and appearance P_{app} of cinnarizine (a decrease of 5.2-fold and 5.0-fold, respectively) was also observed. Cinnarizine appearance P_{app} in the presence of bile and amiloride was therefore not significantly different to that in the absence of bile (and therefore in the absence of supersaturation) (Fig. 4b, Table II). Analysis of the outflowing perfusate in the perfusion experiment suggested that cinnarizine supersaturation was maintained in the bulk GI fluids, in both the absence and presence of amiloride, (*i.e.* precipitation did not occur, Figure S3b). Amiloride co-administration therefore negated the increase in cinnarizine absorption stimulated by bile-mediated supersaturation. Amiloride did not directly influence cinnarizine solubility in model LC colloids in the presence or absence of bile (data not shown).

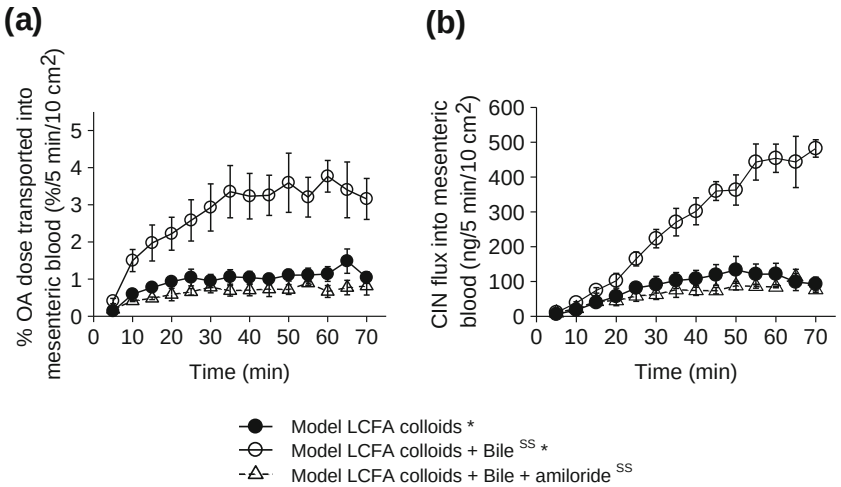

Fig. 4 Absorptive flux-time profiles of (**a**) oleic acid (OA) and (**b**) cinnarizine (CIN) when model LCFA colloids were perfused *via* single-pass through an isolated rat jejunal segment (~ 10 cm^2), with and without 1:1 v/v co-perfusion with donor rat bile, in the absence and presence of 2 mM amiloride. * Data in the absence of amiloride are reproduced from (11). Transport into the mesenteric blood for OA is shown as '% OA dose transported into mesenteric blood' since the concentration of perfused OA in the experimental groups was different. Dose was calculated from the mass of compound contained within the total volume of perfused colloids (*i.e.* 7 mL). Co-perfusion of rat bile generates CIN supersaturation *in situ* within the perfused jejunal segment, and increased cinnarizine absorptive flux by 3.2-fold. Inclusion of 2 mM amiloride in the perfusate, however, abolished the absorption-enhancing effects of bile-induced supersaturation. ^{SS} denotes drug supersaturation in perfusate. Data represent mean ± SEM of $n = 3$–4 rats. Steady state-absorptive flux, disappearance P_{app}, and appearance P_{app} of CIN and OA from this series of experiment are tabulated in Table II.

Table II Cinnarizine (CIN) and Oleic Acid (OA) Disappearance P_{app} ($\times 10^6$ cm/sec) from the Intestinal Perfusate, Appearance P_{app} ($\times 10^6$ cm/sec) in the Mesenteric Blood, and Steady State Absorptive Flux into Mesenteric Blood (ng/5 min/10 cm^2) after 70 min of Single-Pass Perfusion of ~10 cm^2 Segments of Rat Jejunum with Model LCFA Colloids, with and without 1:1 v/v Co-perfusion with Donor Rat Bile, in the Absence and Presence of 2 mM Amiloride. Data in the Absence of Amiloride are Reproduced from (11). Values Calculated Using Data Obtained After Steady State Attainment ($t = 55$–70 min). Data Represent Mean ± SEM of $n = 3$–4 Experiments

	Perfusate	CIN conc. (μg/mL)	OA conc. (μg/mL)	Disappearance P_{app} ($\times 10^6$ cm/sec)	Appearance P_{app} ($\times 10^6$ cm/sec)	Mesenteric blood flux (ng/5 min/10 cm^2)
CIN	LCFA colloid *	65	–	12.2 ± 2.8	0.6 ± 0.2	138 ± 28
	LCFA colloid + Bile ^{SS} *	65	–	36.9 ± 5.5 [a]	2.5 ± 0.2 [a]	443 ± 34 [a]
	LCFA colloid + Bile + amiloride ^{SS}	65	–	52.9 ± 6.3 [a]	0.5 ± 0.0 [b]	85 ± 4 [b]
OA	LCFA colloid *	–	1000	18.0 ± 5.9	2.0 ± 0.3	5607 ± 863
	LCFA colloid + Bile *	–	500	26.1 ± 3.8	6.2 ± 0.8 [a]	8557 ± 1205
	LCFA colloid + Bile + amiloride	–	500	35.0 ± 4.1 [a]	1.4 ± 0.4 [b]	1853 ± 441 [b]

[a] Significantly different ($p < 0.05$) from model LCFA colloid group in the absence of amiloride

[b] Significantly different ($p < 0.05$) from model LCFA colloid + Bile group in the absence of amiloride

* P_{app} and flux data reproduced from (11)

^{SS} denotes drug supersaturation in perfusate, induced by bile dilution of model LCFA colloids

DISCUSSION

The mechanism of absorption of long-chain fatty acid (LCFA) from intestinal mixed micelles is well described in the literature. Westergaard and Dietschy's seminal studies initially proposed that solubilization of LCFA within bile salt micelles increased LCFA diffusion across the intestinal unstirred water layer (UWL), and increased the concentration of LCFA presented to the absorptive membrane (29). Shiau and colleagues later suggested that the acidic microclimate within the UWL further enhanced LCFA absorption by protonating ionized LCFA, leading to enhanced micellar dissociation and absorption (20). These initial studies have also been followed by several studies describing the role of active transport systems such as CD36 (30), FATP (31) and SR-BI (32) in lipid uptake across the apical absorptive membrane, although the quantitative importance of active *vs.* passive transport as a means of lipid absorption under differing lipid loads remains contentious (33–37).

In contrast to lipid absorption, the mechanism of absorption of poorly water-soluble drugs (PWSD) from intestinal mixed micelles is not well defined. We recently described the potential for induction of drug supersaturation during the interaction of lipid colloidal phases (mixed micelles and vesicles) with secreted bile (10,11), and suggested that supersaturation-enhanced absorption may be an endogenous mechanism to reverse the reduction in thermodynamic activity inherent in drug solubilization within colloidal phases. During these studies, however, it became apparent that multiple mechanisms may underpin the generation of drug supersaturation in intestinal mixed micelles. In the current study we have investigated the hypothesis that lipid absorption from intestinal mixed micelles in the acidic UWL reduces drug solubility in micellar structures, thereby inducing supersaturation and promoting drug absorption.

The acidic microclimate associated with the UWL has long been suggested to be important in the absorption of LCFA (20). The pKa of oleic acid, a common LCFA (and digestion product of dietary or formulation-derived lipids), is 9.85 (38). When solubilized in bile salt micelles, however, the pKa of oleic acid decreases to 6.3–6.5 (39). As such pH changes from 6.5 in the GI lumen, to 5.3 in the UWL (17), significantly increase the unionized:ionized fraction for LCFA. A decrease in ionization is expected to increase LCFA absorption by 1) increasing cellular partitioning due to the pH-partition effect and 2) increasing thermodynamic activity due to a reduction in amphiphilicity and micellar solubility, and stimulation of micellar dissociation (19,20). In contrast, conjugated bile salts are not absorbed in the upper GI tract. The pKa values of taurine and glycine conjugated bile salts are <1 and ~3.8, respectively (40). Bile salts therefore remain ionized during passage across the UWL, and in the absence of absorption, bile salt micellar structures are expected to persist. The lipid content of the micelles however, is expected to reduce (due to enhanced LCFA micellar dissociation and absorption), reducing drug solubilization capacity and generating the conditions required for drug supersaturation.

Under pH conditions reflective of the acidic UWL, the LCFA containing colloids examined here became increasingly turbid, suggesting increases in colloid particle size consistent with the observations of Shiau *et al.* (19). The increase in turbidity with decreasing pH only occurred in systems containing LCFA, and developed instantly (see Figure S4 for the appearance of model LCFA colloids after the addition of one drop of 20% v/v H_3PO_4). Reduced LCFA

solubility in bile salt micelles manifests as an increase in system turbidity or phase separation *in vitro*. However, *in vivo* where an absorptive sink is present directly adjacent to the UWL, increased LCFA thermodynamic activity and an increase in unionized:ionized LCFA is expected to contribute to enhanced lipid absorption (19,20). Consistent with this suggestion, the absorptive flux of oleic acid was significantly reduced when the acidic microclimate of the UWL was attenuated by co-administration with amiloride (Fig. 2a). This is consistent with previous data that have shown reduced oleic acid uptake into rat jejunal brush border vesicles in the presence of amiloride (41).

In light of the significant reduction in lipid absorption in the presence of amiloride, this experimental system was utilized to explore the potential link between lipid absorption and drug absorption *i.e.* to probe the effects of suppressed lipid absorption on drug absorption. The data in Fig. 2b show a very clear reduction in cinnarizine absorption in the presence of amiloride (and a reduction in LCFA absorption (Fig. 2a)). In contrast, perfusion of Brij 97 colloids containing the same concentrations of cinnarizine at the same thermodynamic activity resulted in drug flux that was significantly lower than that from LCFA-containing colloids and that was independent of the co-administration of amiloride. The data suggest that drug absorption from micellar systems containing LCFA is inherently more effective than from solubilizing systems that lack fatty acids, and that fatty acid absorption is critical in mobilizing the solubilized fraction to maximize drug absorption. These findings are significant in the context of the design of lipid-based formulations, and suggest that formulations containing absorbable lipids may have inherent advantages over systems containing non-absorbable surfactants and co-solvents. Consistent with this suggestion, previous studies comparing danazol absorption from LBF comprising surfactants and cosolvents alone (*i.e.* LFCS Type IV formulations) and formulations where the same surfactants and cosolvents were combined with glyceride lipids (*i.e.* a more traditional LFCS Type III self-emulsifying formulation), suggest increased drug absorption from the lipid containing formulations (42). Thus, despite similar solubilization properties in *in vitro* dispersion and digestion tests, a glyceride lipid-containing formulation (55% w/w Cremophor RH 40, 7.5% w/w ethanol, 37.5% w/w Soybean oil:Maisine (1:1 w/w)) outperformed (~ 2-fold difference in *in vivo* exposure of danazol) a similar surfactant/cosolvent formulation (55% w/w Cremophor RH 40, 7.5% w/w ethanol, 37.5% w/w Pluronic L121). We were previously unable to explain these observations, but the current studies provide some justification for the apparent advantage of formulations containing absorbable lipids.

As a weak base with a pKa of 7.47, cinnarizine is increasingly ionized at lower pH, and this was reflected in increases in solubility when the pH of blank SEIF (*i.e.* bile micelles with 0% solubilized lipids) and model Brij 97 colloids was decreased from 6.3 to 4.8 (Fig. 3). In LCFA-containing colloids, decreasing pH also resulted in the formation of swollen colloidal particles with increased turbidity and higher cinnarizine solubilization capacity (Fig. 3a), consistent with previous studies that suggest increases in drug solubility in larger colloidal particles (23). The expected changes to cinnarizine solubility resulting from pH changes in the acidic UWL alone (*i.e.* an increase in ionization and solubility, leading to a decrease in thermodynamic activity), are therefore unlikely to promote drug absorption and are unable to explain the *in vivo* data in Fig. 2b. However, a second major change to colloidal structure was expected on entry into the UWL *in vivo*, namely a significant reduction in micellar lipid content due to the promotion of LCFA micellar dissociation and absorption. Since cinnarizine solubility in intestinal colloids is highly dependent on the concentration of incorporated lipids (cinnarizine solubility in LCFA colloids decreased dramatically with decreasing lipid load at each pH studied - Fig. 3a), decreasing lipid concentration is likely to be the predominant factor in determining cinnarizine solubilization at the UWL. Therefore, in predicting the impact of both a decrease in pH and a coincident decrease in micellar lipid concentration in the UWL on drug solubilization (Fig. 3a), the net change to the solubility of cinnarizine in the aqueous phase is likely to be a reduction, due to the loss in lipid content. In the absence of precipitation, this will drive supersaturation and enhance drug thermodynamic activity, consistent with the significant increase in drug flux seen *in vivo* under conditions where lipid absorption was enhanced (Fig. 2a, b).

The ability of the LCFA colloids to harness acidic microclimate-induced drug supersaturation therefore stems from the ability of LCFA to respond to a decrease in pH at the UWL, leading to enhanced LCFA absorption, subsequently decreasing colloid solubilization capacity for PWSD. That is, the presence of oleic acid confers pH sensitivity to LCFA-containing colloids and serves as a trigger for acidic microclimate-induced drug supersaturation, ultimately enabling the absorption of solubilized drug *via* enhancements in thermodynamic activity. Similar events might also be expected for non-ionizable, but absorbable micellar components such as monoglycerides, although in this case, lipid absorption is not stimulated by changes in pH and therefore the effects of acidic microclimate attenuation on drug absorption may not be as significant. Conversely, for colloids that lack an absorbable (and/or pH-responsive) component, potential increases in drug thermodynamic activity due to entry into the acidic microclimate are unlikely, and thermodynamic activity (and absorption) of drug is expected to remain constant (or to decrease as drug is absorbed) during colloidal passage across the UWL. The data obtained here for cinnarizine absorption from Brij 97 colloids (a non-ionizable, non-absorbable surfactant) is consistent with this

suggestion (Fig. 2c). Indeed, when the acidic microclimate was attenuated, and when lipid absorption was effectively inhibited, cinnarizine absorption from LCFA and Brij 97 micelles was comparable and low (Fig. 2b, c). Thus, the data show that the intrinsic solubilization capacity of colloids did not dictate the efficiency of drug absorption; rather, the ability of colloids to lose solubilization capacity and to generate drug supersaturation at the UWL was seemingly more important.

The intercalation of lipid digestion products into bile-derived intestinal colloids has previously been shown to increase solubilization capacity for a range of PWSD (11,15,23,43). Therefore, although cinnarizine was used as a model PWSD in the current study, acidic microclimate-induced drug supersaturation is likely to be a common endogenous mechanism of absorption enhancement for lipophilic PWSD after co-administration with absorbable lipids. The degree of supersaturation that is induced by entry into the acidic microclimate will be dictated by the sensitivity of drug solubility to micellar lipid content, and the efficiency of lipid absorption. Under these circumstances the combination of weak bases, with LBF comprising fatty acids or glyceride that generate fatty acids *in situ*, may be particularly beneficial since the colloid solubility of weak bases in structures containing fatty acids is high (11), and the efficiency of fatty acid absorption is also high.

Previously, we have shown that the interaction of biliary components (*i.e.* bile salts, phospholipid, cholesterol) with similar lipid colloidal phases to those examined here leads to changes in colloid microstructure that dramatically reduce cinnarizine solubilization capacity (10,11). Similar to the events described in the UWL here, precipitation in the previous studies was delayed sufficiently that supersaturation occurred in the bulk luminal fluids and ultimately enhanced the intestinal absorptive flux of cinnarizine. In an attempt to link the current studies at the UWL, with these previous studies that describe luminal supersaturation, a final experiment was performed to explore the importance of a functioning acidic microclimate on increases in drug absorption resulting from supersaturation in the bulk luminal fluids. From the data in Fig. 4b it is apparent that the increase in cinnarizine absorptive flux (that occurred due to interaction of LCFA-containing colloids with bile) was abolished when the acidic microclimate was inhibited with amiloride. It seems likely therefore that even where supersaturation is generated in the intestinal lumen by, for example, initiation of lipid digestion (7,8,15) or interaction with bile (10,11), micellar structures are still required to promote transport across the UWL, and where the micelles contain LCFA, the acidity of the UWL is critical to efficient absorption of LCFA and PWSD. Thus, on approach to the absorptive surface, LFCA protonation and absorption is required to translate luminal supersaturation into enhanced drug absorption, presumably *via* enhancements in thermodynamic activity (that enable drug absorption from the supersaturated solubilized reservoir).

As a final caveat, the generation of drug supersaturation during the processing of LBF is not always expected to be beneficial. Indeed, supersaturation is also a precursor to crystal nucleation and drug precipitation, events that are likely to reduce the absorption of PWSD with dissolution-rate limited absorption. The benefits of supersaturation generation must therefore be weighed against the potential for precipitation. These concepts are expanded in detail in a review in this issue of Pharmaceutical Research (44). However, supersaturation at the UWL may be particularly effective in enhancing drug absorption from intestinal colloids, as proximity to the absorptive membrane is likely to provide an effective sink for removal (*i.e.* absorption) of supersaturated drug, thereby minimizing the risk of drug precipitation. Similar concepts in non-lipid based systems have recently been elegantly exemplified by the Augustijns group where the likelihood of drug precipitation from supersaturated solutions (formed in this case by solvent shift) was dramatically reduced by the presence of an absorptive membrane (45). The viscous, mucus layer that is present at the UWL may also play a role in stabilizing drug supersaturation, as increased viscosity has been suggested to delay nucleation and crystal growth of solutes from supersaturated solutions (46,47).

CONCLUSION

Lipid absorption is an endogenous mechanism that triggers supersaturation for PWSDs and facilitates effective drug absorption from intestinal mixed micelles. Formulations containing absorbable lipids or the pre-digestive precursors to absorbable lipids may therefore be more effective in enhancing PWSD absorption when compared to formulations that lack absorbable components. The degree of drug supersaturation (and therefore absorption enhancement potential) generated by lipid absorption is likely maximized under conditions where the dependency of drug solubility on micellar lipid content is high, and where lipid absorption is highly efficient. Combinations of drug and excipients that are formulated according to the above paradigm (*e.g.* weak bases and lipid-based formulations comprising precursors of fatty acids) may therefore maximize the absorptive benefits associated with lipid absorption-induced drug supersaturation. These data reinforce previous suggestions that lipid-based formulations are able to interact with the dynamic GI environment, and in doing so promote both drug solubilization and thermodynamic activity. This provides unique benefits for drug absorption when compared to formulations that promote solubilization or supersaturation alone. The

data also provide an improved mechanistic understanding of the effects of lipids in food on drug absorption.

ACKNOWLEDGMENTS AND DISCLOSURES

Funding support from the National Health and Medical Research Council (NHMRC) of Australia is gratefully acknowledged.

REFERENCES

1. Williams HD, Trevaskis NL, Charman SA, Shanker RM, Charman WN, Pouton CW, *et al.* Strategies to address low drug solubility in discovery and development. Pharmacol Rev. 2013;65(1):315–499.
2. Porter CJH, Trevaskis NL, Charman WN. Lipids and lipid-based formulations: optimizing the oral delivery of lipophilic drugs. Nat Rev Drug Discov. 2007;6(3):231–48.
3. Poelma FGJ, Breäs R, Tukker JJ, Crommelin DJA. Intestinal absorption of drugs. The influence of mixed micelles on the disappearance kinetics of drugs from the small intestine of the rat. J Pharm Pharmacol. 1991;43(5):317–24.
4. Amidon GE, Higuchi WI, Ho NFH. Theoretical and experimental studies of transport of micelle-solubilized solutes. J Pharm Sci. 1982;71(1):77–84.
5. Miller JM, Beig A, Krieg BJ, Carr RA, Borchardt TB, Amidon GE, *et al.* The solubility–permeability interplay: mechanistic modeling and predictive application of the impact of micellar solubilization on intestinal permeation. Mol Pharm. 2011;8(5):1848–56.
6. Dahan A, Miller JM, Hoffman A, Amidon GE, Amidon GL. The solubility–permeability interplay in using cyclodextrins as pharmaceutical solubilizers: mechanistic modeling and application to progesterone. J Pharm Sci. 2010;99(6):2739–49.
7. Anby MU, Williams HD, McIntosh M, Benameur H, Edwards GA, Pouton CW, *et al.* Lipid digestion as a trigger for supersaturation: evaluation of the impact of supersaturation stabilization on the in vitro and in vivo performance of self-emulsifying drug delivery systems. Mol Pharm. 2012;9(7):2063–79.
8. Williams HD, Anby MU, Sassene P, Kleberg K, Bakala-N'Goma J-C, Calderone M, *et al.* Toward the establishment of standardized in vitro tests for lipid-based formulations. 2. The effect of bile salt concentration and drug loading on the performance of Type I, II, IIIA, IIIB, and IV formulations during in vitro digestion. Mol Pharm. 2012;9(11):3286–300.
9. Williams HD, Sassene P, Kleberg K, Calderone M, Igonin A, Jule E, *et al.* Toward the establishment of standardized *in vitro* tests for lipid-based formulations: 3) Understanding supersaturation *versus* precipitation potential during the *in vitro* digestion of Type I, II, IIIA, IIIB and IV lipid-based formulations. Pharmaceutical Research. 2013. doi:10.1007/s11095-013-1038-z.
10. Yeap YY, Trevaskis NL, Quach T, Tso P, Charman WN, Porter CJH. Bile secretion promotes drug absorption from lipid colloidal phases via induction of supersaturation. Mol Pharm. 2013;10:1874–89.
11. Yeap YY, Trevaskis NL, Porter CJH. The potential for drug supersaturation during intestinal processing of lipid-based formulations may be enhanced for basic drugs. Molecular Pharmaceutics. 2013. doi: 10.1021/mp400035z.
12. Mohsin K, Long MA, Pouton CW. Design of lipid-based formulations for oral administration of poorly water-soluble drugs: precipitation of drug after dispersion of formulations in aqueous solution. J Pharm Sci. 2009;98(10):3582–95.
13. Gao P, Morozowich W. Development of supersaturatable self-emulsifying drug delivery system formulations for improving the oral absorption of poorly soluble drugs. Expert Opin Drug Deliv. 2006;3(1):97–110.
14. Gao P, Rush BD, Pfund WP, Huang T, Bauer JM, Morozowich W, *et al.* Development of a supersaturable SEDDS (S-SEDDS) formulation of paclitaxel with improved oral bioavailability. J Pharm Sci. 2003;92(12):2386–98.
15. Kaukonen AM, Boyd B, Porter C, Charman W. Drug solubilization behavior during in vitro digestion of simple triglyceride lipid solution formulations. Pharm Res. 2004;21(2):245–53.
16. Lucas ML, Schneider W, Haberich FJ, Blair JA. Direct measurement by pH-microelectrode of the pH microclimate in rat proximal jejunum. Proc R Soc London, Ser B. 1975;192(1106):39–48.
17. Shiau YF, Fernandez P, Jackson MJ, McMonagle S. Mechanisms maintaining a low-pH microclimate in the intestine. Am J Physiol Gastrointest Liver Physiol. 1985;248(6):G608–17.
18. Ikuma M, Hanai H, Kaneko E, Hayashi H, Hoshi T. Effects of aging on the microclimate pH of the rat jejunum. Biochim Biophys Acta (BBA) Biomembr. 1996;1280(1):19–26.
19. Shiau YF, Kelemen RJ, Reed MA. Acidic mucin layer facilitates micelle dissociation and fatty acid diffusion. Am J Physiol Gastrointest Liver Physiol. 1990;259(4):G671–5.
20. Shiau YF. Mechanism of intestinal fatty acid uptake in the rat: the role of an acidic microclimate. J Physiol. 1990;421(1):463–74.
21. Li C-Y, Zimmerman CL, Wiedmann TS. Diffusivity of bile salt/phospholipid aggregates in mucin. Pharm Res. 1996;13(4):535–41.
22. Khanvilkar K, Donovan MD, Flanagan DR. Drug transfer through mucus. Adv Drug Deliv Rev. 2001;48(2–3):173–93.
23. Kossena GA, Charman WN, Boyd BJ, Dunstan DE, Porter CJH. Probing drug solubilization patterns in the gastrointestinal tract after administration of lipid-based delivery systems: a phase diagram approach. J Pharm Sci. 2004;93(2):332–48.
24. Mahnensmith RL, Aronson PS. The plasma membrane sodium-hydrogen exchanger and its role in physiological and pathophysiological processes. Circ Res. 1985;56(6):773–88.
25. Williams HD, Sassene P, Kleberg K, Bakala-N'Goma J-C, Calderone M, Jannin V, *et al.* Toward the establishment of standardized in vitro tests for lipid-based formulations, part 1: method parameterization and comparison of in vitro digestion profiles across a range of representative formulations. J Pharm Sci. 2012;101(9):3360–80.
26. Winne D. Rat jejunum perfused in situ: effect of perfusion rate and intraluminal radius on absorption rate and effective unstirred layer thickness. Naunyn Schmiedeberg's Arch Pharmacol. 1979;307(3):265–74.
27. Cummins CL, Salphati L, Reid MJ, Benet LZ. In vivo modulation of intestinal CYP3A metabolism by P-glycoprotein: studies using the rat single-pass intestinal perfusion model. J Pharmacol Exp Ther. 2003;305(1):306–14.
28. Johnson BM, Chen W, Borchardt RT, Charman WN, Porter CJH. A kinetic evaluation of the absorption, efflux, and metabolism of verapamil in the autoperfused rat jejunum. J Pharmacol Exp Ther. 2003;305(1):151–8.
29. Westergaard H, Dietschy JM. The mechanism whereby bile acid micelles increase the rate of fatty acid and cholesterol uptake into the intestinal mucosal cell. J Clin Investig. 1976;58(1):97–108.
30. Nassir F, Wilson B, Han X, Gross RW, Abumrad NA. CD36 is important for fatty acid and cholesterol uptake by the proximal but not distal intestine. J Biol Chem. 2007;282(27):19493–501.
31. Stahl A, Hirsch DJ, Gimeno RE, Punreddy S, Ge P, Watson N, *et al.* Identification of the major intestinal fatty acid transport protein. Mol Cell. 1999;4(3):299–308.

32. Bietrix F, Yan D, Nauze M, Rolland C, Bertrand-Michel J, Coméra C, *et al.* Accelerated lipid absorption in mice overexpressing intestinal SR-BI. J Biol Chem. 2006;281(11):7214–9.
33. Chow SL, Hollander D. A dual, concentration-dependent absorption mechanism of linoleic acid by rat jejunum in vitro. J Lipid Res. 1979;20(3):349–56.
34. Chow SL, Hollander D. Linoleic acid absorption in the unaesthetized rat: mechanism of transport and influence of luminal factors on absorption. Lipids. 1979;14(4):378–85.
35. Ling K-Y, Lee H-Y, Hollander D. Mechanisms of linoleic acid uptake by rabbit small intestinal brush border membrane vesicles. Lipids. 1989;24(1):51–5.
36. Stremmel W. Uptake of fatty acids by jejunal mucosal cells is mediated by a fatty acid binding membrane protein. J Clin Investig. 1988;82(6):2001–10.
37. Goré J, Hoinard C, Couet C. Linoleic acid uptake by isolated enterocytes: influence of α-linolenic acid on absorption. Lipids. 1994;29(10):701–6.
38. Kanicky JR, Shah DO. Effect of degree, type, and position of unsaturation on the pKa of long-chain fatty acids. J Colloid Interface Sci. 2002;256(1):201–7.
39. Hofmann AF. Molecular association in fat digestion. Molecular Association in Biological and Related Systems: American Chemical Society; 1968. p. 53–66.
40. Hofmann AF, Mysels KJ. Bile salts as biological surfactants. Colloids Surf. 1987;30(1):145–73.
41. Schoeller C, Keelan M, Mulvey G, Stremmel W, Thomson ABR. Oleic acid uptake into rat and rabbit jejunal brush border membrane. Biochim Biophys Acta (BBA) Biomembr. 1995;1236(1):51–64.
42. Cuiné JF, McEvoy CL, Charman WN, Pouton CW, Edwards GA, Benameur H, *et al.* Evaluation of the impact of surfactant digestion on the bioavailability of danazol after oral administration of lipidic self-emulsifying formulations to dogs. J Pharm Sci. 2008;97(2):995–1012.
43. Kossena GA, Charman WN, Boyd BJ, Porter CJH. Influence of the intermediate digestion phases of common formulation lipids on the absorption of a poorly water-soluble drug. J Pharm Sci. 2005;94(3):481–92.
44. Williams HD, Trevaskis NL, Pouton CW, Porter CJH. Lipid-based formulations and drug supersaturation: Harnessing the unique benefits of the lipid digestion/absorption pathway. Pharm Res. 2013 (in press, this issue).
45. Bevernage J, Brouwers J, Annaert P, Augustijns P. Drug precipitation–permeation interplay: supersaturation in an absorptive environment. Eur J Pharm Biopharm. 2012;82(2):424–8.
46. Raghavan SL, Trividic A, Davis AF, Hadgraft J. Crystallization of hydrocortisone acetate: influence of polymers. Int J Pharm. 2001;212(2):213–21.
47. Machefer S, Huddar MM, Schnitzlein K. Effect of polymer admixtures on the growth habit of ionic crystals. Study on crystal growth kinetics of potassium dihydrogen phosphate in water/polyol mixtures. J Cryst Growth. 2008;310(24):5347–56.